Title

MICRDSTRUCTURE-ABRASIVE WEAR CHARACTERISTICS OF LOW CARBON DUAL PHASE STEELS

Authors

Kwok, C.K.
Thomas, G.

Publication Date

1984-11-01

Lawrence Berkeley Laboratory
UNIVERSITY OF CALIFORNIA

Materials & Molecular Research Division

Presented at the International Conference
on Wear of Materials, Vancouver, B.C., Canada,
April 14-18, 1985

MICROSTRUCTURE-ABRASIVE WEAR CHARACTERISTICS OF LOW CARBON DUAL PHASE STEELS

C.K. Kwok and G. Thomas

November 1984

Prepared for the U.S. Department of Energy under Contract DE-AC03-76SF00098

DISCLAIMER

MICROSTRUCTURE-ABRASIVE WEAR CHARACTERISTICS OF LOW CARBON DUAL PHASE STEELS

C. K. Kwok and G. Thomas

Department of Materials Science and Mineral Engineering
and Materials and Molecular Research Division,
Lawrence Berkeley Laboratory, University of California,
Berkeley, California 94720

ABSTRACT

Intense plastic deformation due to abrasion is concentrated within a thin surface layer. There are, consequently, extensive microstructural changes from the worn surface to the interior. Microstructural examination of the surface morphology, and the tranverse and longitudinal subsurface areas is necessary to elucidate the relationship between microstructures of the steels and the mode and magnitude of the plastic deformation. Some fundamental entities such as dislocation density, cell size and depth of deformation can be measured or estimated. High voltage transmission electron microscopy has been particularly useful in investigating the wear debris particles. A comprehensive mechanism of abrasive wear has been deduced based on these microstructural observations.

This work was supported by the Director, Office of Energy Research, Office of Basic Energy Sciences, Division of the U. S. Department of Energy under contract number DE-AC03-76SF00098.

1.INTRODUCTION

In order to improve the abrasive wear characteristics of alloys, some basic understanding of its microstructural changes due to abrasion is essential. Most wear systems operate in the microscopic regime, thus, appropriate experimental characterisation methods using such as electron microscopy and Auger electron spectroscopy on debris particles removed by wear and of the worn subsurface is much needed.

Much research of transmission electron microscopy on worn surfaces had been done on pure copper and copper alloys. Previous works [1-6] have shown that a very fine grained polycrystalline or subgrain structure is presented in the heavily deformed region. Similar research on carbon steels [7-11] generated many interesting results, but there is little work [12,13] reported on the microstructural changes of low carbon steels due to abrasive wear.

The aim of this study is to characterize and analyse the microstructure of the worn surface and the nature and origin of the debris of a simple low carbon steel, heat treated to different composite microstructures of two phases..

2.EXPERIMENTAL

2.1 Materials

The low carbon steel chosen in this study was vaccum melted, hot rolled and then hot forged to 15.2mm diameter rod. The nominal composition of the steel is Fe/2.1% Si/0.4% Mn/0.11% C. Two heat treatments were selected to give different microstructures:-

(a) Austenitized at 910^{o} C for 20 minutes and ice-brine quenched to produce a ferritic-martensitic duplex structure with 24%martensite volume fraction (so called "dual-phase"steel[14,15]). The hardness is about 270HV.

(b) Austenitized at 1075^{o} C for 15 minutes and then air cooled to produce a ferritic/pearlitic structure. The hardness is about 195HV.

These samples were examined by standard light optical metallography and their microstructures following these two heat treatments are shown in figures 1.a and 1.b, respectively.

2.2 Wear test

All wear tests were performed at ambient temperature in air without lubrication on a pin-on-disc wear machine under dead load of 2.64N. The pins traversed on 240 grit SiC paper for a total distance of 4.4m at sliding speed of 0.07 m/s. Details of the wear tests can be found in previous work [16].

2.3 Thin foil preparation

Specimens suitable for transmission electron microscopy (TEM) were made as follows:

i) Debris were collected during wear tests by a magnet, and then directly deposited onto a holey carbon grid. Carbon was then vapor deposited over the debris particles.

ii) Nickel-plated worn pins were cut in longitudinal sections, then mechanically polished. The areas containing the wear surface were then electropolished using the window method, with final thinning by liquid nitrogen cold stage ion milling [17].

iii) Thin sections were cut parallel to the worn surface, then the worn surface was covered with lacquer, then jet polishing was done only from the other side until perforation occurred. The lacquer was finally removed using methyl ethyl ketone.

3. RESULTS AND ANALYSIS

3.1 Conventional electron microscopy

The near surface regions where the microstructure was extensively modified during abrasive wear were examined. Figure 2 indicates the relationship between the structures of the debris particle and the subsurface areas for the dual phase steel. The wear pattern observed is typical of the so-called "microploughing" wear, where material is extruded by the blunt abrasive. Dominant material removal process involves microcutting which instantaneous fracture occurred. Secondary fracture due to delamination is also possible [18]. The heavily elongated grains are retained in the debris particle even after the particle is detached from the worn surface. This is commonly observed in other wear particles. From measurements of the grain bending, the critical shear strain in this subsurface region could be in excess of a true strain of 2.5 [19]. The depth of severe deformation varied from 10 um to less than 5 um.

Longitudinal cross-section transmission electron micrographs are shown in figures 2c and 3, from the dual phase steel, and figure 4, from the pearlitic steel. They all show dislocation cells, with a mean thickness of about 30-50nm thick and 2-3um

long. These dislocation cells are elongated immediately beneath the worn surface with well-defined cell boundaries aligned in the direction of abrading. The configuration resembles layers of flat, wide and long slabs. Most of the deformation is concentrated at a narrow region immediately underneath the surface. Microstructure closely resemble non-deformed structure, ferrite and martensite grains with nominal amount of mobile dislocations in the ferrite grains, can be found 3-5 um beneath the worn surface.

On the left hand side of figure 4, a microcrack can be seen to have propagated along the cell boundaries, stopped, and then turned to a new direction to accommodate another packet of dislocation cells running at an angle to the crack propagation path. This may indicate that the grain size of the starting microstructure may have some effect on crack blunting.

Figure 5 shows a plan view of the worn surface of the dual phase steel, after foil preparation from one-side jet polishing, and this gives the identical appearence of the substructure, i.e., dense tangles of dislocations, that can be found in the debris particle (see figure 7). The similarity in substructure suggests that the debris particle is not different from the surface before the final separation. Using similar assumptions to those of Adlers and Vasamillet [20],(foil thickness ~300nm and limit of resolution of individual dislocation ~10nm), a lower bound estimate of the dislocation density is on the order of 10^{11} lines/cm^2. This is a very large density typically of very high strained metals and alloys, for example, after explosive deformation or maretensitic transformation.

3.2 High voltage transmission electron microscopy

i) Debris analysis

The size, shape, composition and distribution of debris particles can give important clues to their origin and nature. Hundreds of debris particles were collected and examined in a scanning electron microscope from which it was found that more than 75% of the wear particles are in the form of "machining" chips [21], they are long and slender with aspect ratio usually larger than 1:5 and mean thickness on the order of 1um (see figure 6). However, the particle thickness could vary over a large range from 0.2 μm to over 10 μm. Some of the less commonly found but nonetheless important wear particles are in the form of chunks or flakes which are formed by microploughing [20] (see figure 2). One very important point is that after intense plastic deformation, there is almost no distinction between wear particles of different starting microstructures (either ferrite/martensite or ferrite/pearlite) as both will attain the same final microstructure (see figures 6 and 7).

For a conventional 100keV electron beam, the maximum pentration for a ferrous alloy is about 200 - 300nm. But since

most debris particles have thickness > 1 μm, through thickness observation is difficult. One of the advantages of using the high voltage (1.5 MV) electron microscope is the quadruple improvement of electron penetration and no thinning of the wear particles is required for many cases [22]. The structure of the debris particle from the dual phase steel is shown in figure 7a; it consists of dense dislocation tangles in a very fine grained structure. A dark field micrograph (figure 7b) taken from a segment of the {110} diffraction ring indicates a fine grain size on the order or 30-50nm. The corresponding selected area diffraction pattern consists of fairly uniform bcc diffraction rings. No extra oxide diffraction ring was found.

One of the salient features of wear particles that exhibit "machining chip" characteristics is the segmentation of the debris into a lamellar structure as evidenced in figure 6 and figure 8. The lamellar structure, as suggested by Ramalingam and Black [23], is a result of a thermally activated shear process. Since adiabatic shear involves a high temperature generated at a very narrow shear front, a thermally activated microstructural changes such as recovery, recrystallization or even melting could occur.

However, careful investigation along this lamellar boundaries (as enclosed by the box in figure 8a) does not reveal any microstructural change between this narrow region and the other areas in the debris.

Based on this observation, thermal softening by high temperature is not a priori a prerequisite for chip formation in this wear system and further study is required to clarify this instability problem.

ii) In situ recovery/recrystallization experiment

The similarity in microstructure of the debris particles and the area immediately below the newly deformed worn surface is discussed in section 3.1. This finding implied that no, or minor, stress relief occurs after the debris particle is detached from the worn surface. These wear debris particles retained a deformation strain greater than 2 and so should recover/recrystallize if external thermal energy is provided. It is interesting to understand the kinetics of recovery/recrystallization of these debris particles.

Figure 8 is a series of time-sequence bright field micrographs with corresponding selected area diffraction patterns, taken at times after 2 minutes, 9 minutes and 24 minutes heating. The debris particle was collected from a wear test run on the dual phase steel pin, and the hot-stage experiment was done directly in the electron microscope.

In this experiment, the temperature rose uniformly and rapidly from room temperature to 400° C within 30 seconds. After 9 minutes of heating, the temperature was further increased to 600° C within 20 seconds to encourage accelerated recrystallization.

Before heating, the starting microstructure of the wear

particle was composed of small (20-50nm) cells with high dislocation density (figure 8a). Selected area diffraction (figure8b) of almost continous ring pattern suggested a very fine grain size with a large range of misorientations.

After one minute heating at 400°C, dislocations inside the cells start to migrate to cell walls and some of the dislocations are observed to escape to the free surface by climb. Figure 8d and 8b appear to be very similar which indicates that subgrain coalescence has not taken place after 2 minutes at 400°C.

After 9 minutes, small dislocation-free grains appeared (circled in figure 8e) suggesting the start of recrystallization. Small carbides also started to precipitate. Then, when the temperature is increased to 600°C, after 15 minutes, it appears that recrystallization is almost completed and some grain growth has occurred. Spherodized cementite particles can also be found at the final stage of annealing (at arrowed in figure 8f). The dislocation density shown in figure 8f is very much lower compared to that in figure 8e. The corresponding electron diffraction pattern gives a single [111] spot diffraction pattern, indicating a single grain. The beam size for all the diffraction patterns taken in figure 8 is about 0.1μm.

The investigation of the annealing response of debris particles in the "as-collected" condition is more realistic than using bulk specimens or ex-situ annealing experiment because of the size effect and the difficulty of duplicating the same deformation strain.

Even after annealing the wear particles at 600°C, the microstructural change (thermal softening) does not occur instantaneously. This result may imply the way in which the material responds to rapid localized heating during abrasion.

3.3 Auger electron spectroscopy

Auger electron spectroscopy (AES) is a powerful tool for determining the composition of solid surfaces. It offers excellent depth resolution and light element (Z >2) detectability. Thus, it is particularly useful to investigate the oxidative nature of the debris particles. Based on Evans et al's estimation [24], iron particles with specific area (area/mass) greater than 0.8 m^2/g spontaneously oxidized at 285°C. Since the specific area of most debris particles collected in this study falls in this range (for example, a typical debris particle with dimension 20μm x 2μm x 0.3 μm has specific area of about 1.0), thus, through-thickness oxidation could occur if the local temperature is higher than 250°C around these particles.

AES studies have been performed on many small particles yielding similar spectra. Two typical Auger spectra are shown in figure 9a and 9b. Figure 9a represents the composition spectrum of the debris surface and figure 9b represents the interior (about 140 nm from the original surface) after 2 minutes of Argon ion sputtering. Figure 10 is an iron/oxygen depth profile plot

showing the relative amount of iron and oxygen peaks against the sputtering time. This result shows that the oxygen content decreases rapidly in the first 10-15 seconds and becomes very low after 15 seconds sputtering (comparable to the oxygen background noise). This depth profile indicates that the oxide layer on the wear debris surface is no more than 15nm thick which is about normal for ambient oxide formation on ferrous alloys.

Quantitive analysis of a debris particle is made by comparing the peak to peak measurements from the first derivative of the Auger spectra of the debris particles with that from a pure silver specimen and then using the known sensitivity factors relative to silver [25]. The accuracy of such measurements is typically around 20%. But for this multi-component system the accuracy may be poorer. Nevertheless, it is still worthwhile to look for large differences in oxygen content of the debris surface. The amount of oxygen on the surface and in the interior after 2 minutes sputtering are 2.0 weight percent and 0.3 weight percent, respectively. The low oxygen content of the debris particle indicates no excessive oxidation has taken place which is well in accord with the electron diffraction evidence discussed previously (figure 7). Thus, it can be inferred that the temperature rise in the lameller structure may not be higher than 250°C.

A substantial amount of carbon is found in the top spectrum. This could possibly be due to the presence of the absorbed layer of hydrocarbon on the surface, or minute fragments of silicon carbide attached to the debris. Also, a trace of carbon monoxide could exist in the scanning Auger microscope.

4. SUMMARY AND CONCLUSIONS

Based on the above metallographic observations, a simple model of abrasive wear in these steels can be proposed. At the onset of abrasion, indentation is made by an abrasive particle, and when the tangential load exceeds the local yield strength, the material has to flow around and under the abrasive particle. The dislocation density increases very rapidly to accommodate the large shear plastic strain component. Dislocations tangle and cluster into cell walls to reduce the strain energy. These dislocation cells elongate in the direction of abrasion and some cell rotations may occur. Cell walls become the sources and the sinks of further dislocation multiplication.

A typical cell resembles a long, flat and wide slab [26], and the worn surface region is built up by stacking of these slabs of dislocation cells. Assuming a cutting mode is operating, fracture would occur when the critical shear strain is exceeded. The critical shear strain, can be estimated from a grain bending method. Dislocation cell boundaries may have the large strain gradient due to crystallographic mismatch, which could promote microcrack nucleation as the critical shear strain is exceeded. Microchip formation then involves propagation of these cracks along cell boundaries to eventually separate material from the surface, leaving behind a shallow layer of cell

structure. The debris particle should then be composed of a very fine dislocation cell structure containing very high dislocation density as is in fact obsrved. For low carbon steels of the same composition but different starting microstructures, the final microstructures found in both the subsurface regions and the debris particles appear to be identical.

The temperature effect on chip formation may play only a secondary role as microstructural changes due to frictional heat are rarely observed in these experiments. This is quite different from the sliding wear results which recovery zone is found immediately underneath the deformed surface [27].

ACKNOWLEDGEMENTS

The authors wish to thank Mr. D.Ackland and Ms. E.Fong for technical assistance and Nippon Kokan K.K. for supplying the alloys used in this study. This work was supported by the Director, Office of Energy Research, Office of Basic Energy Science, Division of the U.S. Department of Energy under the contract number DE-AC03-76SF00098.

REFERENCES

1. N.Ohmae,T.Tsukizo and F.Akiyama,Phil.Mag.,40,pp.803 (1979)
2. D.Turley and L.Samuels,Metallography,14,pp.275 (1981)
3. J.VanDijck,Wear,42,pp.109 (1977)
4. J.Dautzenberg,Wear,60,pp.401 (1980)
5. R.Bill and D.Wisander,Wear,41,pp.351 (1977)
6. L.Ives,"Proc. Wear of material,1979",pp.246.
7. A.Torrance and A.Cameron,Wear,28,pp.299 (1974)
8. S.Hogmark and O.Vingsbo,Wear,38,pp.341 (1976)
9. K.Fujita and A.Yoshida,Wear,43,pp.301 (1977)
10. J.Pearce,Wear,89,pp.333 (1983)
11. J.Edington and I.Wright,Wear,48,pp.145 (1978)
12. K.Nakajima and Y.mizutani,Wear,13,pp.283 (1969)
13. I.Garbar and J.Skornin,Wear,51,pp.327 (1978)
14. J.Koo and G.Thomas,Met.Trans.,8A,pp.525 (1977)
15. G.Thomas and J.Koo,"Structure and Properties of dual phase steels" pp.183 (AIME, 1979)
16. C.Kwok and G.Thomas,"Proc. Wear of materials,1983",pp.140.
17. S.Hogmark, H.Swahn and O.Vingsbo,Ultramicroscopy,1,ppl13 (1975)
18. N.Suh,Wear,25,pp.111 (1973)
19. J.Duatzenberg and J.Zaat,Wear,23,pp.9 (1973)
20. M.Adler and L.Vasamillet,J.of App.Phys,39,pp.3592 (1968)
21. K-H. Zum Gahr,"Proc. Wear of materials 1979",pp.266
22. G.Thomas and M.Goringe,"Transmission Electron Microscopy of Materials" (J.Wiley & Sons,N.Y.,1979)
23. S.Ramalingam and J.Black,Met Trans.,4,pp.1103 (1973)
24. J.Evans,W.Borland and P.Mardon,Pow.Met.,1,pp.17 (1976)
25. L.Davis, et al,"Handbook of Auger Electron Spectroscopy" (Perkin-Elmer, 1976)
26. D.Rigney and W.Gleaser,Wear,46,pp.241 (1978)
27. W.Salesky,R.Fisher,R.Ritchie and G.Thomas,"Proc. Wear of Materials,1983",pp.434.

FIGURE CAPTIONS

Figure 1. Optical metallographs showing (a) dual phase ferrite/martensite (b) ferrite/pearlite structure. The pearlite (the dark phase) is too fine to be resolved.

Figure 2. (A) and (B), SEM micrographs of substructure region and debris particle, respectively. (C) Longitudinal cross-section TEM shows dislocation cells. Material is dual phase steel.

Figure 3. TEM of longitudinal section. The steel is in dual phase condition.

Figure 4. TEM of longitudinal section shows microcrack propagation along the cell boundary in abraded pearlitic steel.

Figure 5. TEM of parallel section shows substructure of the dual phase steel resembling that of the debris particle collected in the same wear test.

Figure 6. (a) and (b) are SEM images of machining chips, (c) and (d) are TEM images of machining chips showing a lamellar structure. The wear chips were collected from abraded pearlitic steel.

Figure 7. (a) Bright field, (b) dark field from segment of the (110) ring and (c) SAD of debris indicating the presence of a fine grain size,in the dual phase steel.

Figure 8. (a),(c),(e) and (f) are bright field micrographs showing recovery and recrystallization after heating in-situ. (b),(d) and (g) are the corresponding SAD. (dual phase steel).

Figure 9. Auger spectra of dual phase steel debris particle (a) before and (b) after 2 minutes sputtering.

Figure 10 .Iron and Oxygen depth profile (collected from the same particles as in figure 9) during 2 minutes of Argon ion sputtering. One minute sputtering corresponds to roughly 70 nm of material removed from the original surface.

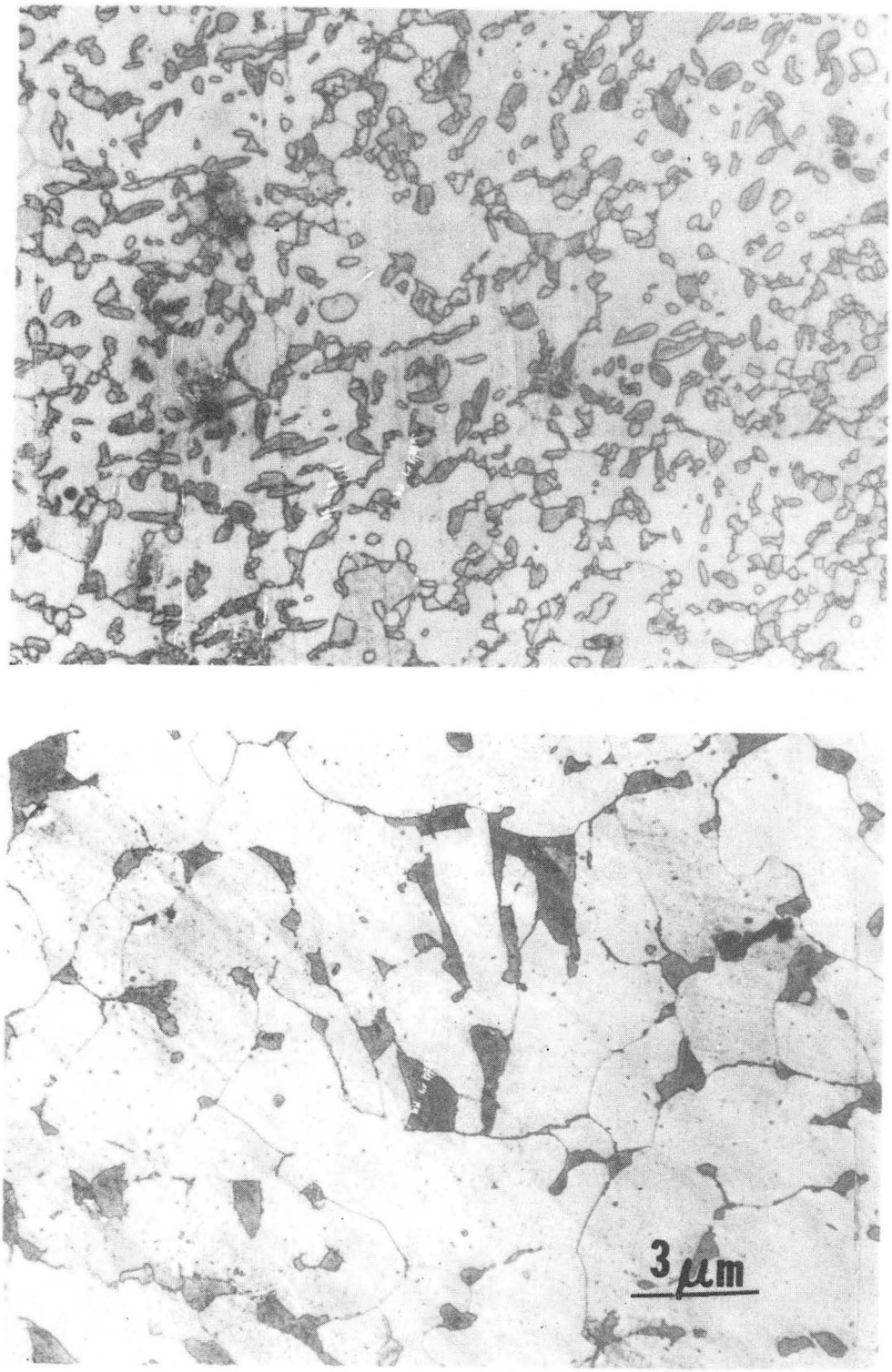

Fig. 1 XBB 847-5498

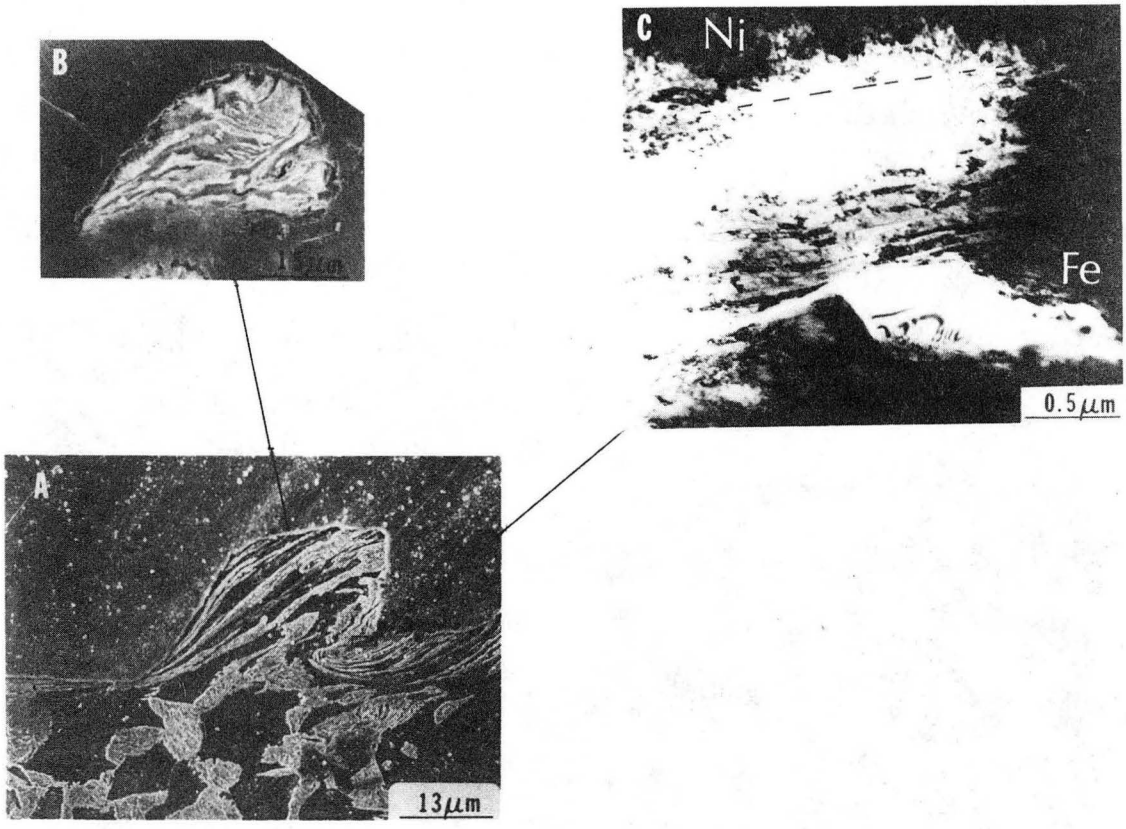

XBB 820-10906

Fig. 2

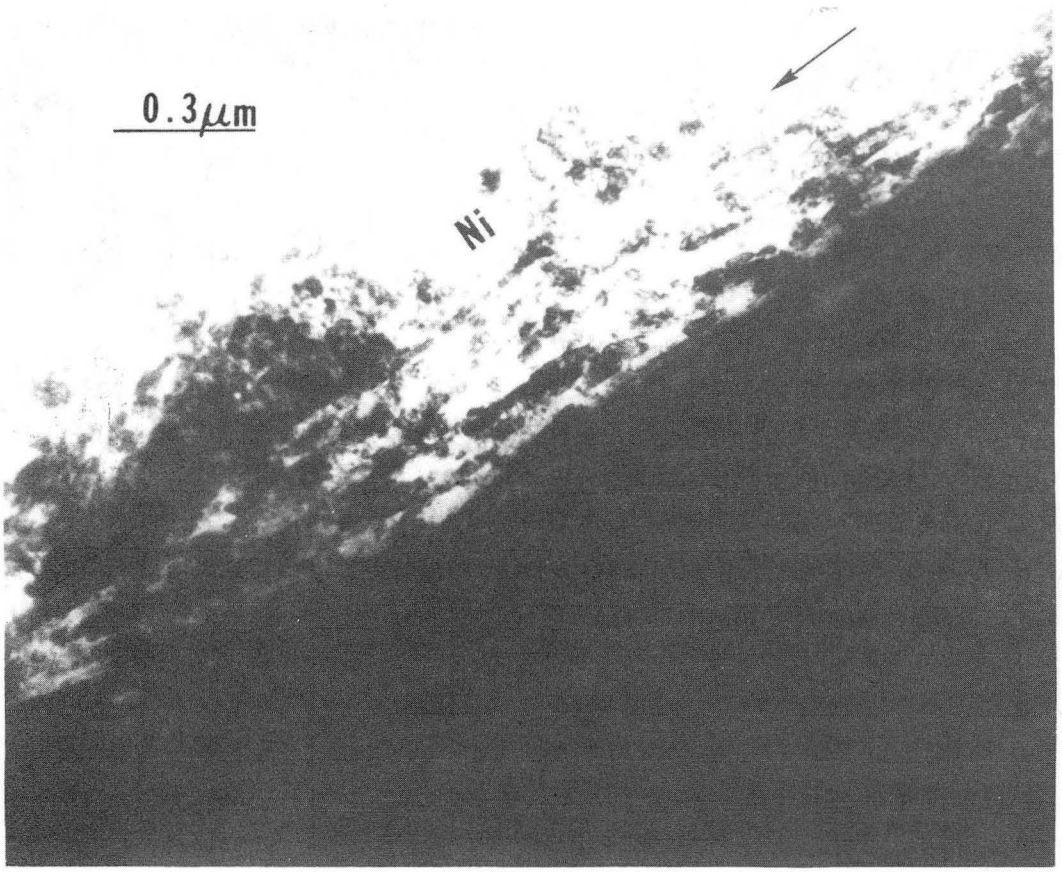

Fig. 3 XBB 830-10230

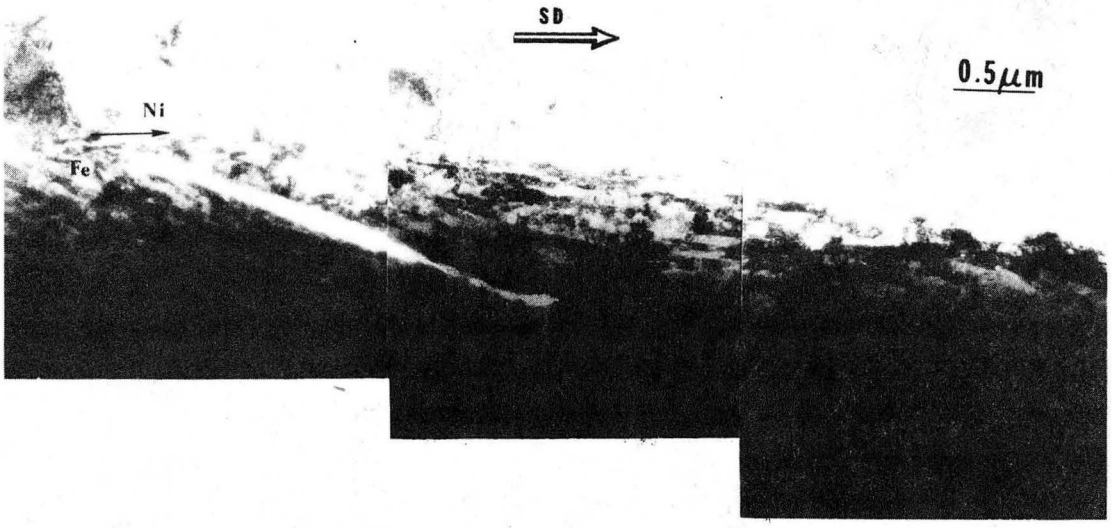

Fig. 4 XBB 847-5500

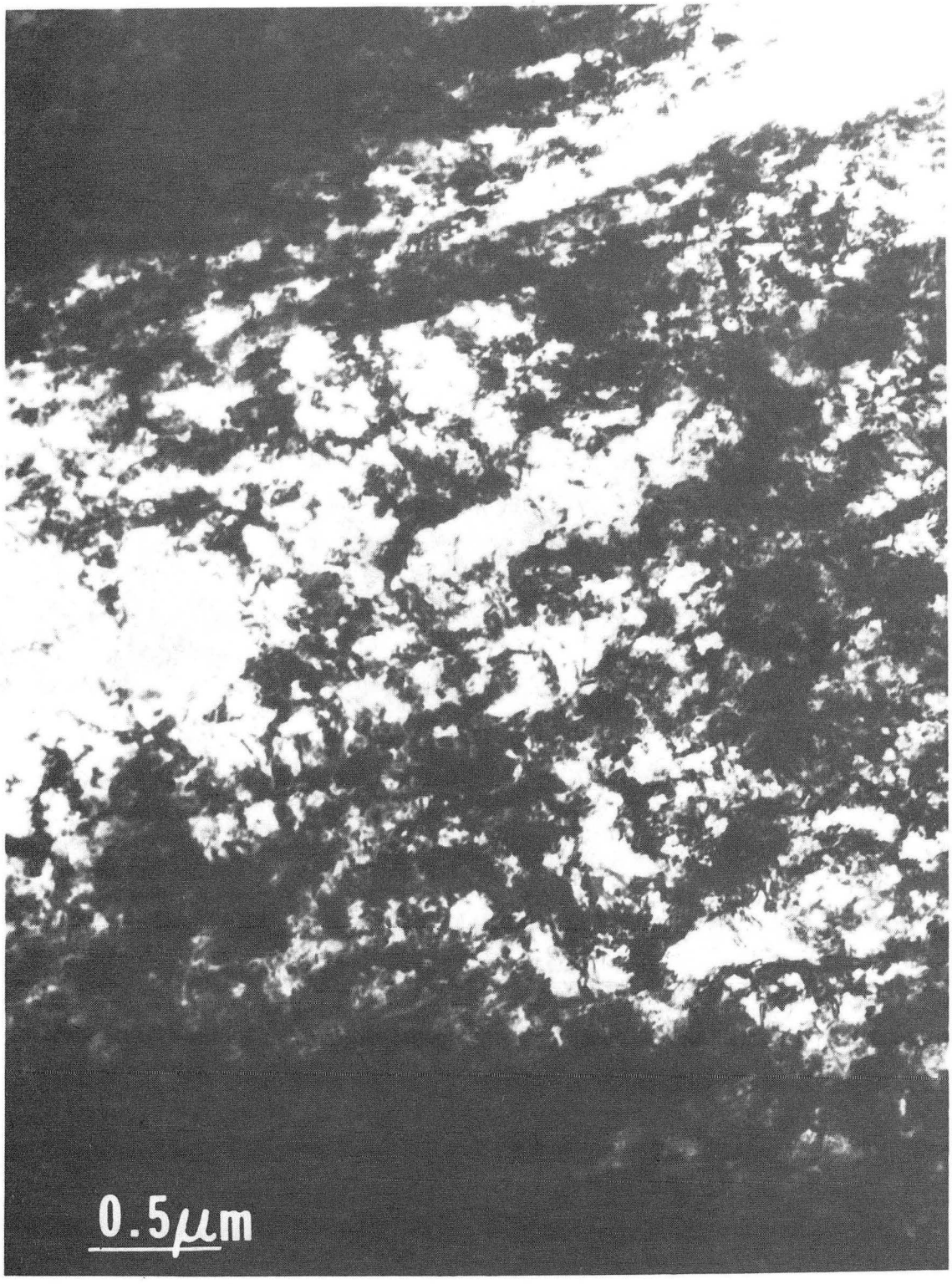

Fig. 5 XBB 840-9572

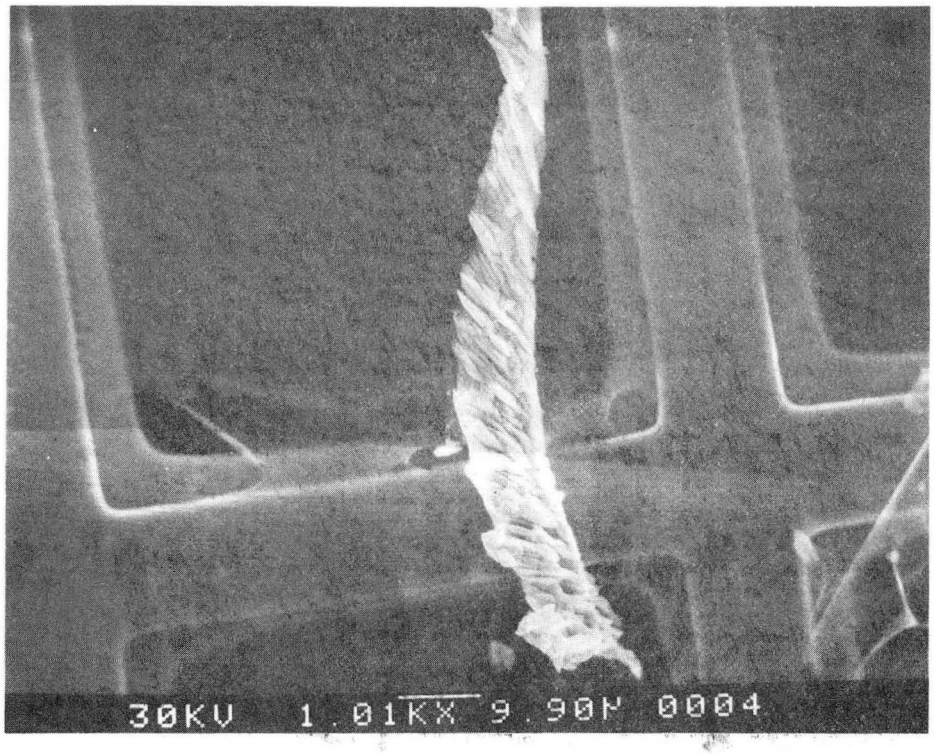

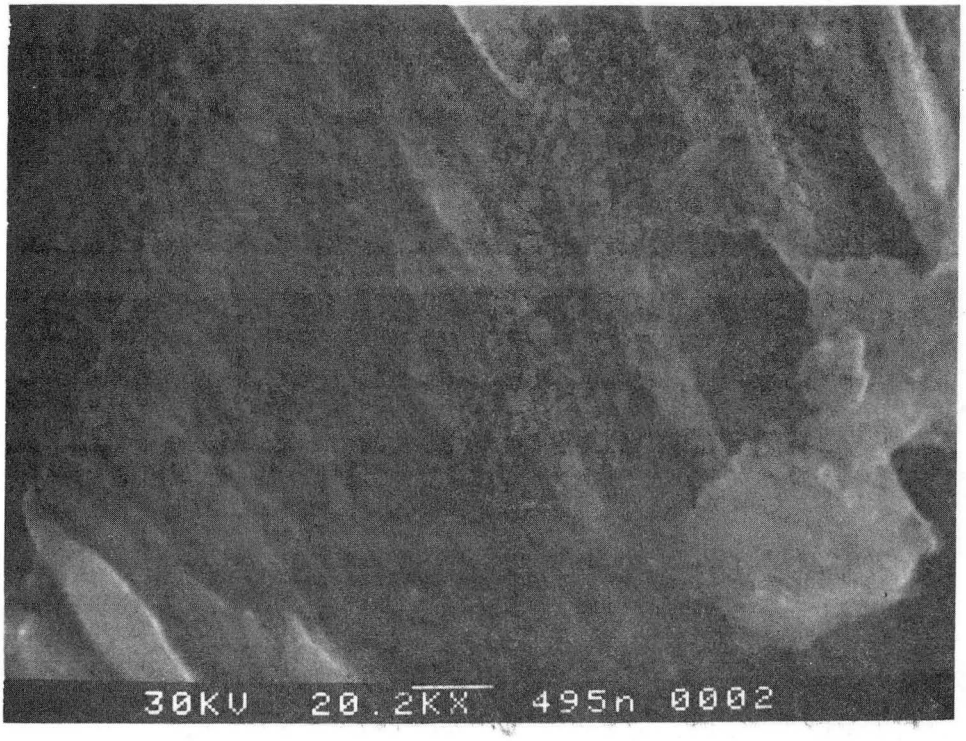

Fig. 6
(a) & (b)

XBB 847-5497

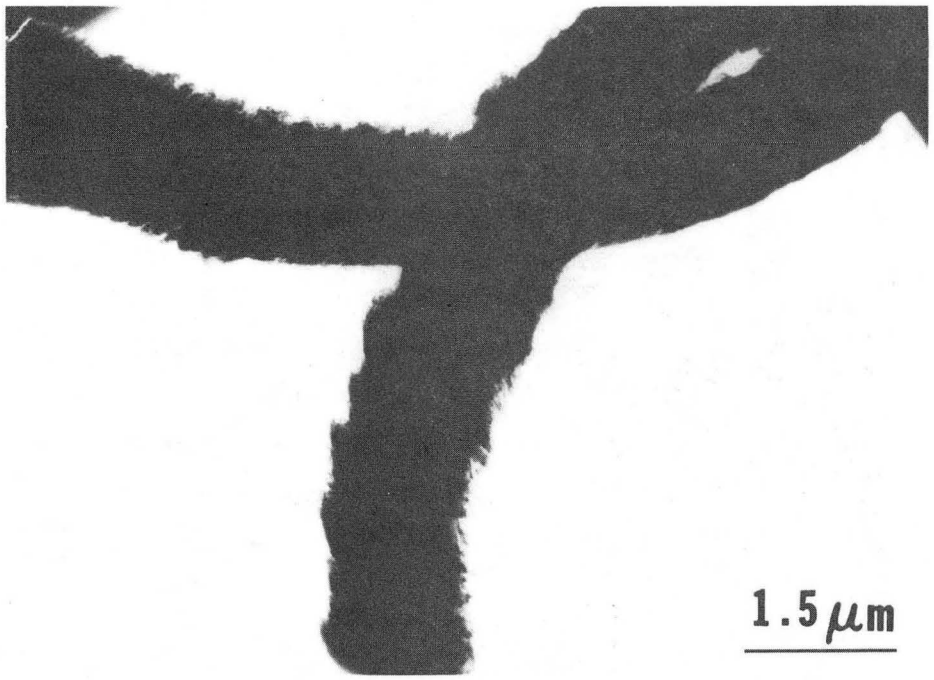

XBB 847-5499

Fig. 6
(c) & (d)

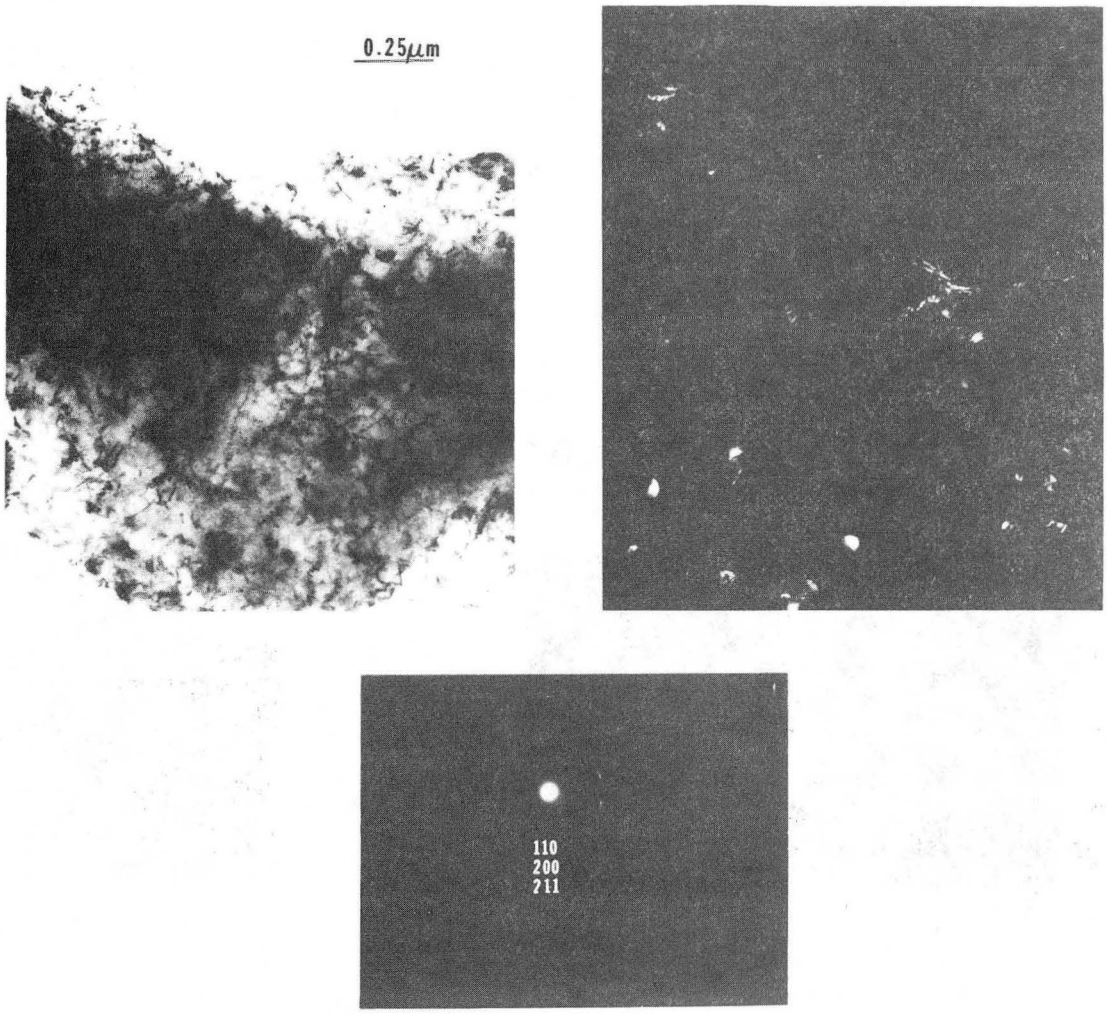

Fig. 7 XBB 830-10233

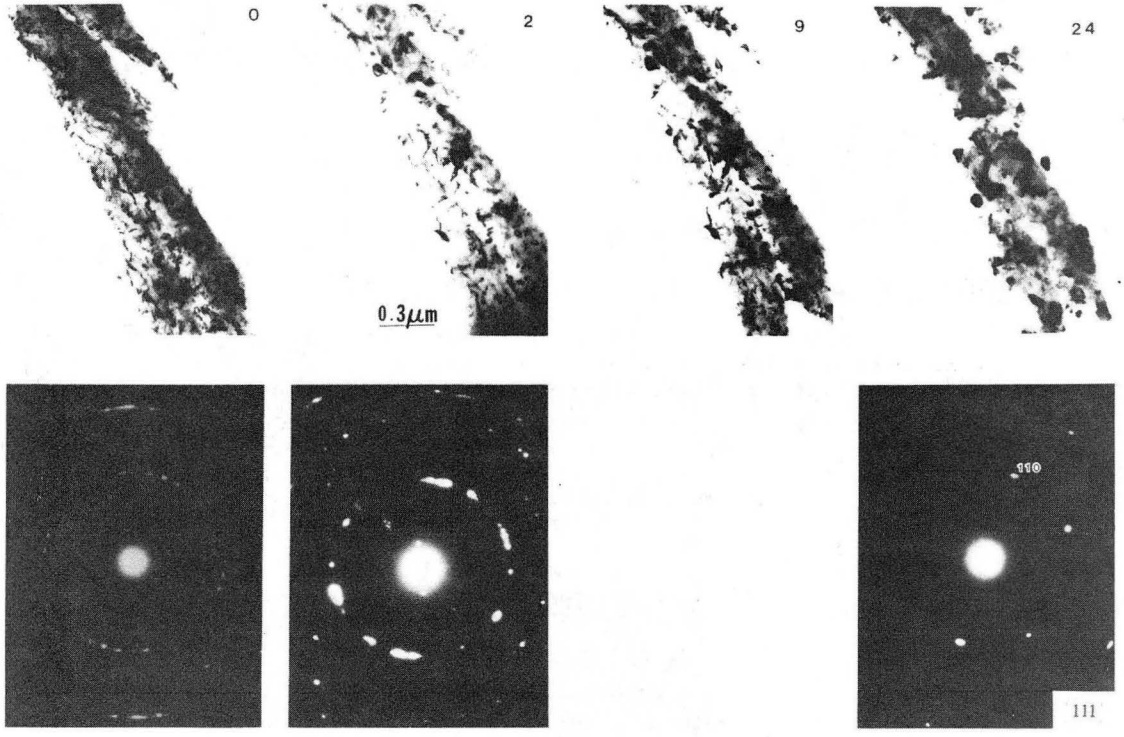

Fig. 8

XBB 847-5501

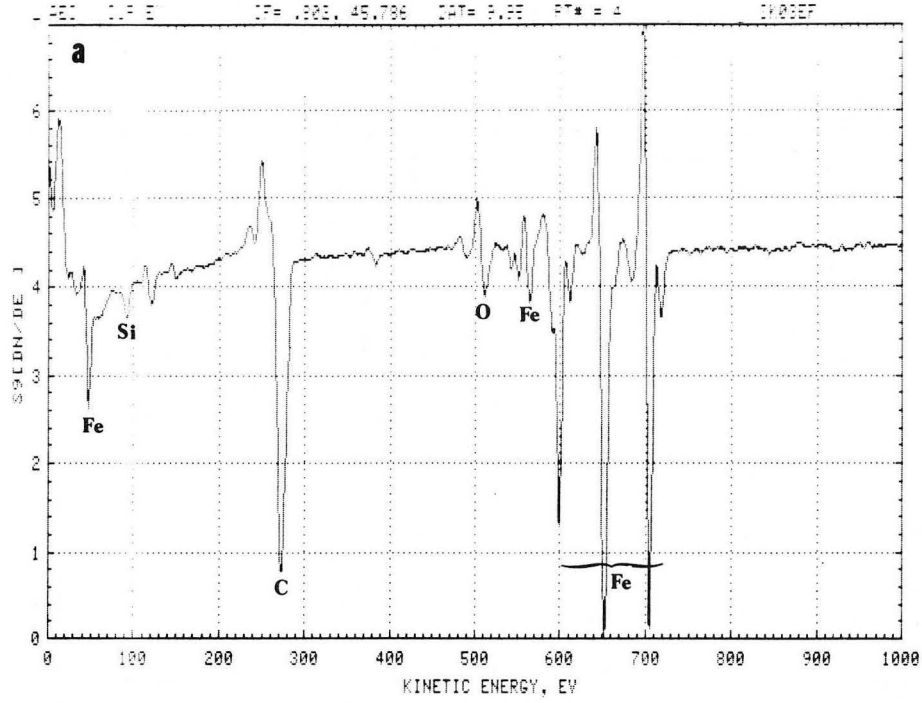

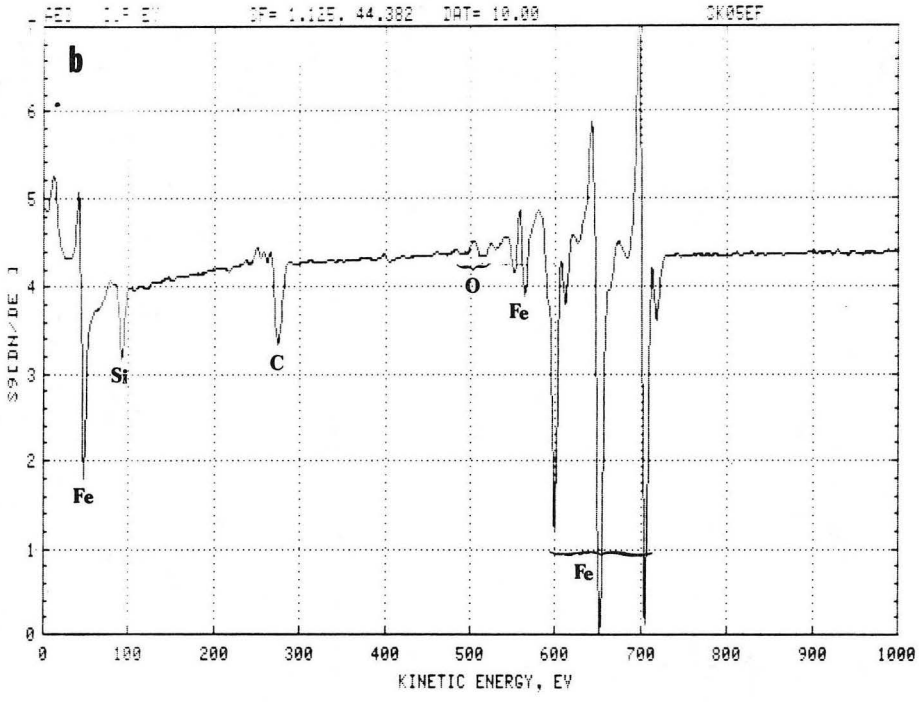

XBL 848-3314

Fig. 9

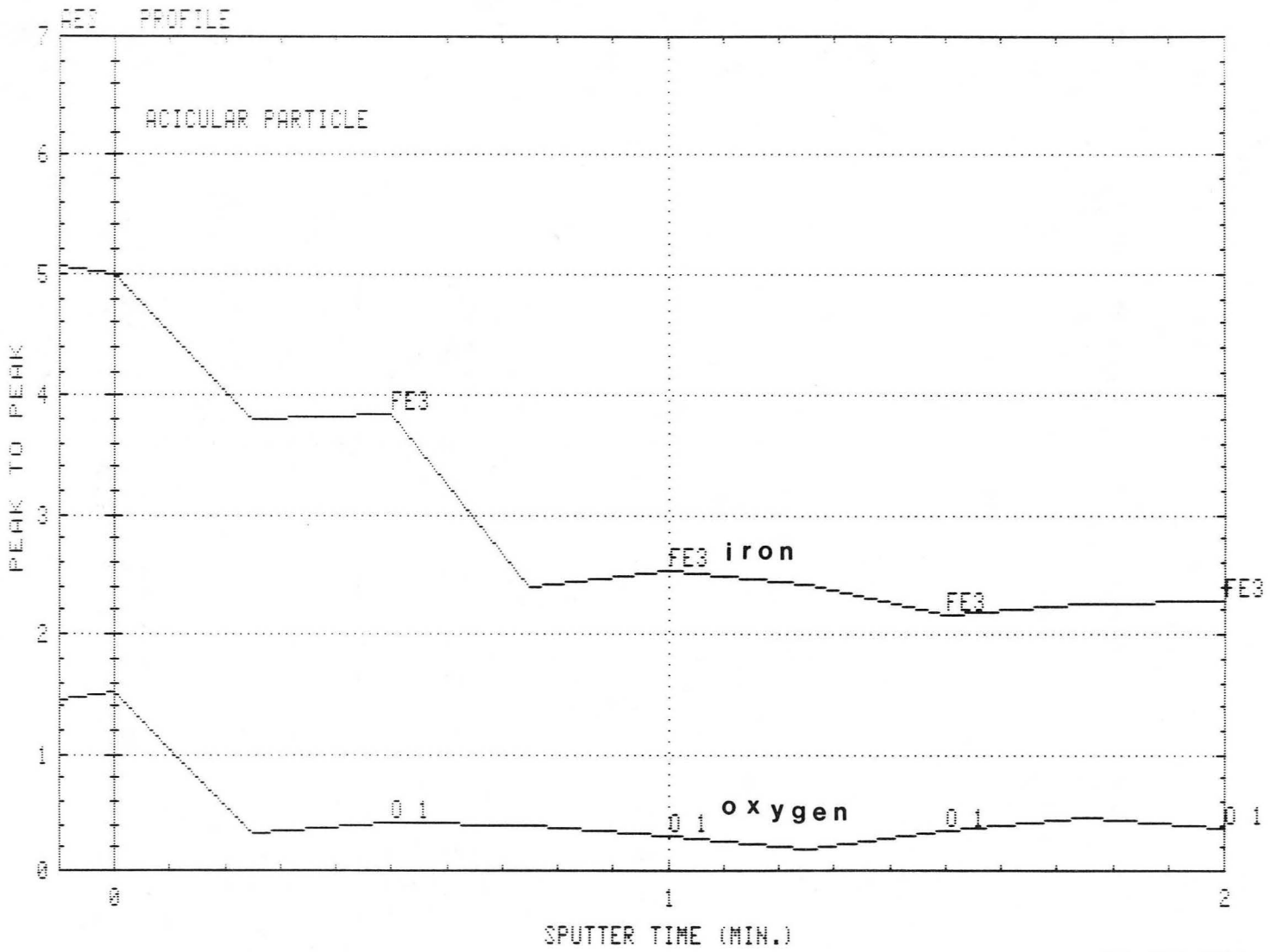

XBL 851-1014

Fig. 10

TECHNICAL INFORMATION DEPARTMENT
LAWRENCE BERKELEY LABORATORY
UNIVERSITY OF CALIFORNIA
BERKELEY, CALIFORNIA 94720